esa

ECOSPHERE

Rhizosphere priming effects in soil aggregates with different size classes

XIAOHONG WANG,[1,2] FEIKE A. DIJKSTRA,[3] LIMING YIN,[1,†] DI SUN,[1] AND WEIXIN CHENG[4]

[1]*CAS Key Laboratory of Forest Ecology and Management, Institute of Applied Ecology, Chinese Academy of Sciences, Shenyang, China*

[2]*University of Chinese Academy of Sciences, Beijing 100049 China*

[3]*School of Life and Environmental Sciences, Sydney Institute of Agriculture, The University of Sydney, Sydney, New South Wales 2570 Australia*

[4]*Environmental Studies Department, University of California, Santa Cruz, California 95064 USA*

Citation: Wang, X., F. A. Dijkstra, L. Yin, D. Sun, and W. Cheng. 2020. Rhizosphere priming effects in soil aggregates with different size classes. Ecosphere 11(2):e03027. 10.1002/ecs2.3027

Abstract. The change in native soil organic carbon (SOC) decomposition caused by plant roots or the rhizosphere priming effect (RPE) is a common phenomenon. Although most of the SOC is stored in aggregates with different size classes, the RPE in aggregates and the underlying mechanisms remain unclear. In a 35-d pot experiment, we grew *Agropyron cristatum* (C_3 plant) in pots containing large macroaggregates (LMA), small macroaggregates (SMA), and microaggregates (MA) separated from a C_4 soil. We quantified the RPE and measured microbial biomass C (MBC), oxidase activity, soil net nitrogen (N) mineralization, and aggregate dynamics at the end of the experiment. The positive RPEs ranged from 47% to 106% and were significantly lower in the SMA treatment than in the LMA and MA treatments. Planting significantly increased microbial N immobilization in all treatments, particularly in the SMA treatment. Furthermore, the positive relationship between RPE and plant-induced changes in net N mineralization suggests that increasing microbial N immobilization could reduce RPE. Planting significantly increased MBC and oxidase activity, and the positive relationships between SOC decomposition and MBC and oxidase activity suggest that microbial activation may play an important role in the positive RPEs. Planting significantly reduced aggregate destruction in the SMA treatment but increased aggregate destruction in the MA treatment, supporting the aggregate destruction hypothesis. Overall, our results showed for the first time that the RPEs varied among aggregate size classes, with potentially important consequences for SOC dynamics in soils that have a high capacity for aggregation.

Key words: aggregate destruction; microbial biomass C; net N mineralization; oxidase activity; plant growth.

Received 12 March 2019; revised 21 July 2019; accepted 3 December 2019. Corresponding Editor: Kristofer D. Johnson.

† **E-mail:** limingyin@iae.ac.cn

INTRODUCTION

Soil organic carbon (SOC) is the largest C pool in terrestrial ecosystems, and small fluctuations in SOC decomposition can cause a drastic variation in atmospheric CO_2 concentration (Bond-Lamberty and Thomson 2010, Lehmann and Kleber 2015). One of the pivotal mechanisms for the fluctuation is the priming effect, particularly, the rhizosphere priming effect (RPE), that is, the change in native SOC decomposition caused by plant roots (Cheng et al. 2014). Recent syntheses and experiments showed that the RPE can retard SOC decomposition up to 50% or accelerate it up to 455% (Cheng et al. 2014, Yin et al. 2019). Therefore, the RPE (especially the positive RPE that is often observed) has been increasingly considered as a pivotal

component of the ecosystem feedback to climate change (Finzi et al. 2015, Huo et al. 2017).

Although numerous studies have focused on the potential factors influencing the RPE (Cheng et al. 2014), the effect of soil aggregates (structure) is still unknown. As summarized in Cheng et al. (2014), the factors can be classified into plant- and soil-derived variables. For the plant variables, for example, plant biomass and root-derived CO_2 (which tend to relate positively to the quantity of rhizodeposits) have been found to be positively related to the RPE (Dijkstra et al. 2006, Zhu and Cheng 2013, Shahzad et al. 2015, Yin et al. 2018), while plant N acquisition has also been observed to be significantly related to the RPE (Dijkstra et al. 2009, Lu et al. 2018, Yin et al. 2018). However, less attention has been paid to soil variables (Dijkstra and Cheng 2007, Zhu and Cheng 2013). Particularly, there is a knowledge gap with regards to soil aggregates (structure; Cheng et al. 2014). Soil aggregates, which not only influence microbial accessible substrates through physical protection, but also influence microbial biomass distribution and activity, plant growth, and nutrient acquisition (Six et al. 2004), may therefore cause different RPEs.

There are potentially different mechanisms by which aggregate size class can influence RPEs. Firstly, aggregate size class can alter plant growth and N acquisition (Donald et al. 1987, Alexander and Miller 1991, Passioura 1991) and consequently influence RPE through altering the release and diffusion of rhizodeposits and soil N mineralization. The release of rhizodeposits as a readily available C and energy source can stimulate microbial activation and subsequently increase enzyme activity, leading to increased decomposition of native SOC (Cheng and Kuzyakov 2005). Furthermore, plant N acquisition can lead to competition for N between plants and microbes, thereby influencing plant growth and rhizodeposition (Murphy et al. 2017, Lu et al. 2018). If a high proportion of available N derived from an RPE-induced increase in N mineralization is re-immobilized by microbes rather than taken up by plants, that is, microbial net N immobilization, the RPE may be slowed down (Lu et al. 2018, Yin et al. 2018).

Secondly, aggregates with different size classes differ in microbial activities. Microbes may benefit from the higher quantity and quality of SOC and the limited protection in macroaggregates (Tisdall and Oades 1982, Jastrow et al. 2007), resulting in higher microbial biomass and enzyme activity compared to microaggregates (Dorodnikov et al. 2009, Gupta and Germida 2015). Therefore, rhizodeposition (labile C) may cause different responses in microbial activities among different aggregates and thus different RPEs. For example, Kumar et al. (2017) found that planting significantly increased MBC in the large macroaggregates while hydrolytic enzyme activities increased in microaggregates.

Thirdly, aggregates with different size classes differ in physical stability (Rabot et al. 2018), which can lead to different dynamics (destruction and formation) in response to the disturbance of living roots (Six et al. 2004). The destruction of macroaggregates caused by living roots may release previously protected C, resulting in a positive RPE, that is, the aggregate destruction hypothesis (Cheng and Kuzyakov 2005). However, microaggregates are hard to disrupt due to their higher stability and smaller size, but often bind together to build macroaggregates by living roots (De Gryze et al. 2005). This information suggests that there may be different RPEs in microaggregates relative to macroaggregates.

Overall, our main goal of this study was to investigate whether there is a difference in RPEs in aggregates with different size classes and to determine the possible reasons behind potential differences. We hypothesized that (1) planting would cause positive RPEs and that the RPEs may vary among aggregates with different size classes; (2) the positive RPE would be positively related to plant growth, plant-induced changes in net N mineralization, and microbial activities; and (3) the RPE would be higher in the treatment where planting increased aggregate destruction than in the treatment where planting increased aggregate formation or stabilization. To accomplish this goal and verify these hypotheses, we conducted a 35-d pot experiment by growing a C_3 plant (*Agropyron cristatum*) in pots filled with large macroaggregates (LMA), small macroaggregates (SMA), and microaggregates (MA), respectively. These soil aggregates were separated from a C_4 soil using a wet-sieving method (Elliott 1986).

Materials and Methods

Soil and experiment design

The experimental soil (C_4 soil, with a ^{13}C value of −20.54‰) was collected from the plow layer (0–20 cm depth) of a field soil continuously cropped for 23 yr with maize at the experimental station of Heilongjiang Academy of Agricultural Sciences located near Harbin, Heilongjiang Province. This C_4 soil was sieved through a 4-mm screen to homogenize and remove organic residues and other fragments.

The C_4 soil was separated into three size classes of water-stable aggregates by a wet-sieving method (Elliott 1986), including large macroaggregates (LMA), small macroaggregates (SMA), and microaggregates (MA). Briefly, 60 g air-dried soil samples were placed on top of a stack of sieves (1-mm and 0.25-mm aperture sieves) and submerged in water for 5 min. Then, we manually moved the sieves up and down for 50 repetitions in 2 min. The materials remaining on the 1-mm and 0.25-mm sieves were transferred into separate beakers, oven-dried at 50°C, and weighed, representing the LMA (>1 mm) and SMA (0.25–1 mm) fraction, respectively. Material smaller than 0.25 mm was allowed to settle, centrifuged, and oven-dried at 50°C, representing the MA (<0.25 mm) fraction. Total N content, SOC content, C:N ratio, and mineral N content of these aggregates were measured on a elemental analyzer (Elementar III, Langenselbold, Germany), and initial values are shown in Table 1.

Six treatment combinations were designed: three aggregate size classes (LMA, SMA, and MA) either with or without plants. There were four replicates for each treatment; a total of 24 pots were used in this experiment: 12 pots were unplanted, and another group of 12 pots was planted with the C_3 grass *Agropyron cristatum*. Briefly, a sandbag filled with 50 g sand was placed at the bottom of each polyvinyl chloride (PVC) pot (5 cm in diameter, 15 cm in height, fitted with an inlet tube at the bottom for aeration and CO_2 trapping). We then carefully filled each PVC pot with 250 g dried soil aggregates of certain size. All pots were watered with deionized water to 60% soil water-holding capacity (equivalent to 18.8% gravimetric soil moisture content) and maintained at this soil moisture content throughout the experiment by daily watering. In the planted treatment, we sowed four seeds of *Agropyron cristatum* and thinned to two plants per pot after seedlings emerged. Anaerobic conditions in all pots were prevented by forcing ambient air into the soil for 10 min every 6 h with an aquarium air pump and a digital timer. The experiment was conducted for 35 d in a greenhouse with air temperature ranging from 15°C to 35°C.

CO_2 trapping

We measured soil respiration of each treatment at 35 d after planting (DAP35) by a CO_2 trapping method (Keith et al. 2015) with some modifications. Briefly, we sealed each pot with nontoxic silicone rubber on the soil surface with a flexible plastic tube (3 cm depth) protruding through the seal. After testing for air leakage, a soda lime column, a pump, a needle valve, and a one-way valve were connected to the tube at the bottom of each pot in sequence to remove the CO_2 inside the pots for 1 h. Then, CO_2 produced in each pot during a 48-h period was trapped by connecting a CO_2 trapping bottle with 22 mL of 0.5 M NaOH solution and an airstone for producing fine air bubbles. During CO_2 trapping, the air inside the soil–roots system was circulated for 15 min every 3 h using pumps controlled by a digital timer, and the air-flow rate was kept at

Table 1. Initial values of total N (TN, g/kg aggregate), soil organic C (SOC, g/kg aggregate), C:N ratio, and $\delta^{13}C$ (‰) in the three aggregate treatments at the start of the experiment.

Treatment	TN	SOC	C:N ratio	$\delta^{13}C$
LMA	1.45 ± 0.01 b	17.51 ± 0.28 b	12.10 ± 0.23 a	–20.03 ± 0.12 b
SMA	1.52 ± 0.01 a	18.55 ± 0.16 a	12.22 ± 0.20 a	–20.64 ± 0.09 a
MA	1.36 ± 0.02 c	15.74 ± 0.09 c	11.61 ± 0.18 a	–20.90 ± 0.06 a

Notes: LMA, large macroaggregates; SMA, small macroaggregates; and MA, microaggregates.
Different lowercase letters indicate significant differences in the same column ($P < 0.05$). Values represent mean ± SE; $n = 3$ for each size of aggregate.

90–100 mL/min controlled by the needle valve. We also used three extra pots with plants to measure ^{13}C isotopic fractionation (Wang et al. 2016). We removed whole soils from the pots and cleaned roots carefully by washing. Then, each plant was planted into pots with 250 g glass beads (0.25–0.3 mm diameter) and added water. We used the same CO_2 trapping method as mentioned above. An aliquot of each NaOH solution was analyzed for total inorganic C using a multi N/C 2000 TOC analyzer (Analytik, Jena, Germany). Another aliquot was analyzed for $\delta^{13}C$ using cavity ring-down spectroscopy (CRDS) with the Automate Module (Picarro G2131-i Analyzer, Picarro, Santa Clara, California, USA).

Measurements after harvest

Immediately after CO_2 trapping, plant shoots were cut off at the soil surface. In order to reduce the effects of destructive sampling on aggregates, the soil was slipped out by gently beating the pot with a hammer, and then, roots were collected carefully by hands, without destructing soil aggregates, that is, using a 4-mm screen. Shoots and roots were cleaned and oven-dried at 60°C for 48 h and weighed, and then ground by a ball mill for C and N analyses on an elemental analyzer (Elementar III). Soil samples were homogenized for measuring soil moisture, microbial biomass carbon (MBC), potential extracellular enzyme activity, and water-stable aggregates immediately after harvesting.

Moisture, microbial biomass carbon (mg C/kg soil) was measured by the chloroform fumigation-extraction method (Vance et al. 1987). Briefly, 20 g fresh soil was fumigated with ethanol-free chloroform for 24 h; then, fumigated and non-fumigated soils were extracted with 60 mL 0.05 M K_2SO_4. The extracts were measured for total organic C (TOC) using the multi N/C 2000 TOC analyzer. Moisture, microbial biomass carbon was calculated as the difference in TOC between fumigated and non-fumigated soil extracts with a conversion factor of 0.45. Soil mineral N (sum of NH_4^+ and NO_3^-) in treatments at the start (initial) and at the end of the experiment (final) was measured by extracting 20 g fresh soil with 40 mL of 2 M KCl solution and was analyzed for NH_4^+ and NO_3^- on a continuous flow analyzer (AA3, Bran + Luebbe, Norderstedt, Germany).

Two oxidative enzymes were measured using the fluorogenically labeled substrates method (Zhu et al. 2014). Briefly, phenol oxidase (PO) and peroxidase (PER) activity were measured with L-3, 4-dihydroxyphenylalanine as a substrate. 1.5 g fresh soil was dispersed by thoroughly mixing in 125 mL buffer (50 mM Tris, pH = 6.7 according to soil pH). Then, 50 μL aliquots were dispensed in 96-well microplates (Brand pure Grade, black), followed by appropriate standards, homogenates, and substrates. Microplates were placed in the dark at 20°C for 24 h, and the absorbance was measured at 460 nm wavelength on a microplate reader (BioTek Synergy HT MultiMode; BioTek Instrument, Winooski, Vermont, USA). Oxidase activity (PO + PER) was expressed in $\mu mol \cdot g^{-1}$ soil$\cdot h^{-1}$.

Calculations

We calculated soil-derived CO_2 (C_{soil}, mg $C \cdot kg^{-1}$ soil$\cdot d^{-1}$) by using a two-source mixing model (Cheng et al. 2003):

$$C_{soil} = C_{total} \times (\delta^{13}C_{root} - \delta^{13}C_{total})/(\delta^{13}C_{root} - \delta^{13}C_{soil}) \quad (1)$$

$$C_{root} = C_{total} - C_{soil} \quad (2)$$

where $\delta^{13}C_{total}$ is the measured $\delta^{13}C$ value of total soil respiration, $\delta^{13}C_{soil}$ is the mean $\delta^{13}C$ value of soil-derived CO_2 in the unplanted treatment, and $\delta^{13}C_{root}$ is the $\delta^{13}C$ value of root-derived CO_2 in the planted treatment, which was calculated by adding the $\delta^{13}C$ value caused by isotopic fractionation (mean ± standard error: −1.96 ± 0.32‰) to the $\delta^{13}C$ value of root biomass. We calculated the $\delta^{13}C$ fractionation (‰) as the difference between $\delta^{13}C$ values in CO_2 produced from the rhizosphere and root biomass of the plants transplanted into pots with glass beads.

The RPE was calculated as the difference in soil-derived CO_2 between planted and unplanted treatments, and the magnitude of the RPE (%) was quantified as follows:

$$RPE = [C_{soil(planted)} - C_{soil(unplanted)}]/C_{soil(unplanted)} \times 100 \quad (3)$$

Based on the plant N acquisition and mineral N remaining in soil, we calculated net N

mineralization rate (N_{net}, mg $N \cdot kg^{-1}$ aggregate$\cdot d^{-1}$) during the 35-d period as follows (Dijkstra et al. 2009):

$$N_{net} = \left[N_{acq} + N_{soil(final)} - N_{soil(initial)}\right]/\Delta time \quad (4)$$

where N_{acq} is plant N acquisition, that is, the sum of N content in shoot and root biomass, $N_{soil\ (final)}$ and $N_{soil\ (initial)}$ are the soil mineral N content at the end and start of the experiment, respectively, and Δtime is the time interval, that is, 35 d. For the planted treatments, we also calculated the plant-induced changes in net N mineralization by subtracting the average net N mineralization rate in the unplanted control from the net N mineralization rate in the corresponding planted treatment (Dijkstra et al. 2009).

Statistical analysis

One-way ANOVA with a Turkey-Kramer honest significant difference (HSD) test was used to assess the effect of aggregate size on plant shoot, root, and the ratio between them; ^{13}C of shoot and root; plant N uptake; RPE; and soil properties of aggregates. Two-way ANOVA was used to assess the effects of planting, aggregate size and their interaction on soil-derived CO_2, MBC, oxidase activity, and mineral N. *t*-Test was used to compare the aggregate amount between the unplanted control and planted treatment. Simple linear regression was used to examine the relationships between soil-derived CO_2 and MBC and oxidase activity, and between primed net N mineralization and primed C across all treatments. All statistical analyses were performed by SPSS Statistic 20.0, and the significance level was set at $P < 0.05$. Origin 8.5 was used to create figures.

Results

Chemical properties in each aggregate size class

The total N and SOC in each aggregate size class significantly decreased from SMA to MA at the beginning of the experiment ($P < 0.05$, Table 1), while there was no significant difference in C:N ratio ($P > 0.05$). The $\delta\ ^{13}C$ value was slightly higher in LMAs than in SMAs and MAs with the largest difference being less than one per mil ($P < 0.05$, Table 1).

Plant biomass, shoot:root ratio, and $\delta\ ^{13}C$ value

Shoot and root biomass of *Agropyron cristatum* were on average 64% and 19% higher in the SMA treatment than in the MA and LMA treatments, respectively ($P < 0.05$, Table 2). Shoot:root ratio was on average 39% higher in the LMA treatment than in the other two aggregate treatments ($P < 0.05$, Table 2).

Root-derived CO_2, Soil-derived CO_2, and RPE

Root-derived CO_2 was on average 51% higher in the MA treatment than in the LMA and SMA treatments ($P < 0.05$, Fig. 1a). Soil-derived CO_2 was similar among aggregate size classes in unplanted controls or in planted treatments ($P > 0.05$). Planting significantly increased soil-derived CO_2 compared to the unplanted controls (i.e., positive RPEs). The RPE, ranging from 47% to 106%, was on average 117% lower in the SMA treatment than in the other treatments ($P < 0.05$, Fig. 1b).

Plant N acquisition, soil mineral N, net N mineralization

At harvest time, plant N acquisition ranged from 25 to 40 mg N/kg aggregate and significantly decreased with a decrease in aggregate size ($P < 0.05$, Fig. 2a). Compared to the mineral N in the unplanted controls (with a range of 32–53 mg N/kg aggregate), planting drastically decreased the mineral N by 93% on average, particularly in the SMA treatment where the mineral N was decreased by 96% (planting × aggregate size class, $P < 0.05$, Fig. 2b). Net N mineralization was mostly negative, except for the LMA treatment without plants, which suggests

Table 2. Plant shoot and root biomass, shoot:root ratio, and their $\delta^{13}C$ values in the three aggregate treatments at the end of the experiment.

Size	Shoot	Root	Shoot:root ratio
Biomass (g/kg aggregate)			
LMA	0.93 ± 0.05 b	0.57 ± 0.05 c	1.66 ± 0.09 a
SMA	1.24 ± 0.04 a	1.09 ± 0.04 a	1.14 ± 0.02 b
MA	1.10 ± 0.05 ab	0.87 ± 0.01 b	1.27 ± 0.07 b

Notes: Different lowercase letters indicate significant differences in the same column ($P < 0.05$). Values represent mean ± SE; $n = 4$ for each size of aggregate. For the abbreviations of soil aggregates, please see Table 1.

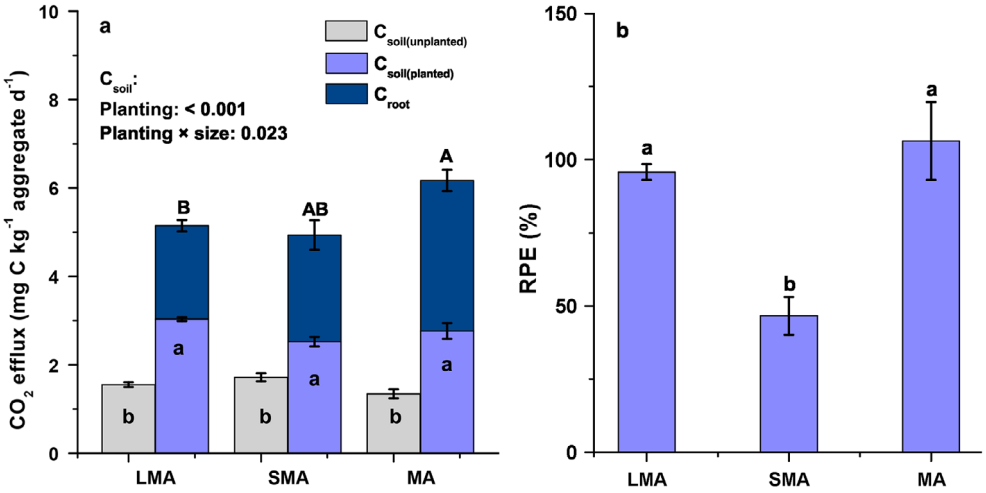

Fig. 1. CO_2 efflux of soil-derived CO_2 and root-derived CO_2 (a) and the magnitude of the rhizosphere priming effect (RPE, %, b) in the three aggregate treatments with or without planting. Two-way ANOVA *P*-values are shown when significant ($P < 0.05$), and planting and size represent the main effect of planting and aggregate size class, respectively. Different lowercase letters indicate significant differences in soil-derived CO_2 (including planted or unplanted treatments) or RPE among aggregate size classes; different uppercase letters indicate significant differences in root-derived CO_2 among aggregate size classes ($P < 0.05$). Error bars indicate standard errors of the mean, $n = 4$ for each treatment. For the abbreviations of soil aggregates, please see Table 1.

microbial net N immobilization (Fig. 2c). Further, net N mineralization was more negative in the planted treatments than in the corresponding unplanted controls, particularly in the SMA treatment (planting × aggregate size class, $P < 0.05$, Fig. 2c). In the planted treatments, the plant-induced changes in net N mineralization were significantly more negative in the SMA treatment than in the LMA and MA treatments ($P < 0.05$, Fig. 2d).

Microbial biomass C and oxidase activity

Moisture, microbial biomass carbon slightly decreased with decreasing aggregate size class in the unplanted controls ($P > 0.05$). Compared to the unplanted controls, planting significantly increased MBC by 46% on average, particularly in the MA treatment (increase of 87%; planting × aggregate size, $P < 0.05$, Fig. 3a). Oxidase activity increased with decreasing aggregate size class in the unplanted controls ($P > 0.05$, Fig. 3b). Compared to the unplanted controls, planting significantly increased oxidase activity by 129% on average, particularly in the LMA treatment (increase of 272%; planting × aggregate size class, $P < 0.05$, Fig. 3b).

Aggregate size redistribution

Each aggregate treatment was initially comprised by their sole aggregate size, but was finally redistributed into several size classes (Fig. 4). Compared to the initial percentage (100%), the average loss of LMA and SMA was 82% and 72% percent in the corresponding treatments, respectively (Fig. 4a, b), while the change in the percentage of MA in the MA treatment was small, both in planted and in unplanted treatments (Fig. 4c). Compared to the unplanted control, planting did not cause a significant change in aggregate size redistribution in the LMA treatment (Fig. 4a), but significantly increased the percentage of SMA by 30% in the SMA treatment (Fig. 4b) and significantly but weakly decreased the formation of SMA in the MA treatment (Fig. 4c).

Relationships between variables

We found a significant positive relationship between the plant-induced changes in net N mineralization and RPE in the planted treatments ($R^2 = 0.36$, $P = 0.04$, Fig. 5a) and significant positive relationships between the soil-derived CO_2 and MBC ($R^2 = 0.55$, $P < 0.01$, Fig. 5b) and

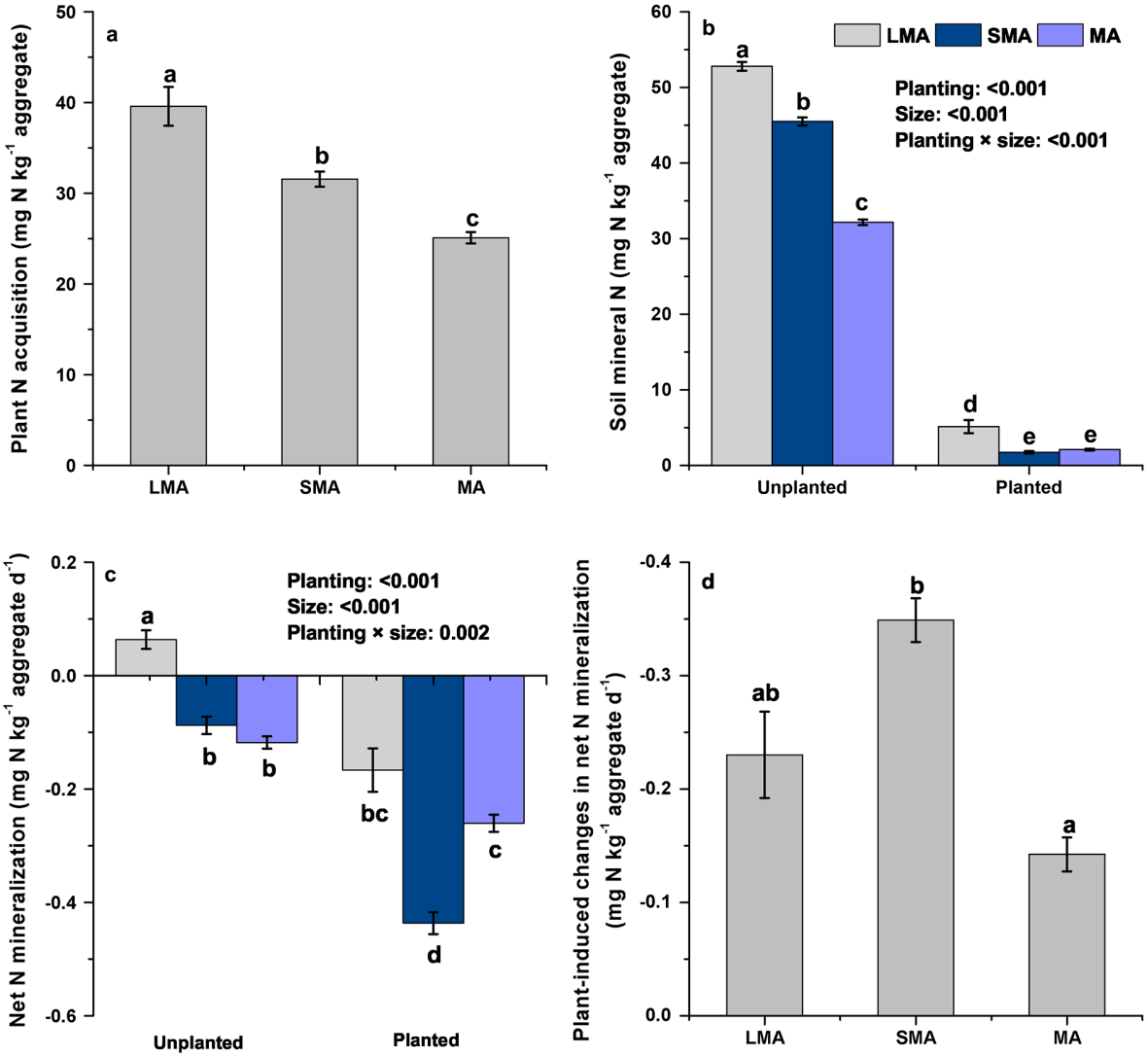

Fig. 2. Plant N acquisition (a), soil mineral N content (b), net N mineralization (c), and excess net N mineralization (d) in the three aggregate treatments with or without planting at the end of the experiment. Two-way ANOVA *P*-values are shown when significant ($P < 0.05$), and planting and size represent the effect of planting and aggregate size, respectively. Different lowercase letters indicate significant differences across all aggregates ($P < 0.05$). Error bars indicate standard errors of the mean, $n = 4$ for each treatment. For the abbreviations of soil aggregates, please see Table 1.

oxidase activity across all treatments ($R^2 = 0.55$, $P < 0.01$, Fig. 5c).

Discussion

Variation in RPEs among aggregate size classes

In the current study, RPEs were measured in aggregates with different size classes by growing *Agropyron cristatum*. The range of RPEs (47–106%) obtained in these aggregates was within the range (−50% to 380%) summarized by Cheng et al. (2014) and similar to values reported in recent studies using grass species (Shahzad et al. 2015, Lu et al. 2018, 2019). RPEs in different aggregates were studied in the current study because aggregates play a key role in storing

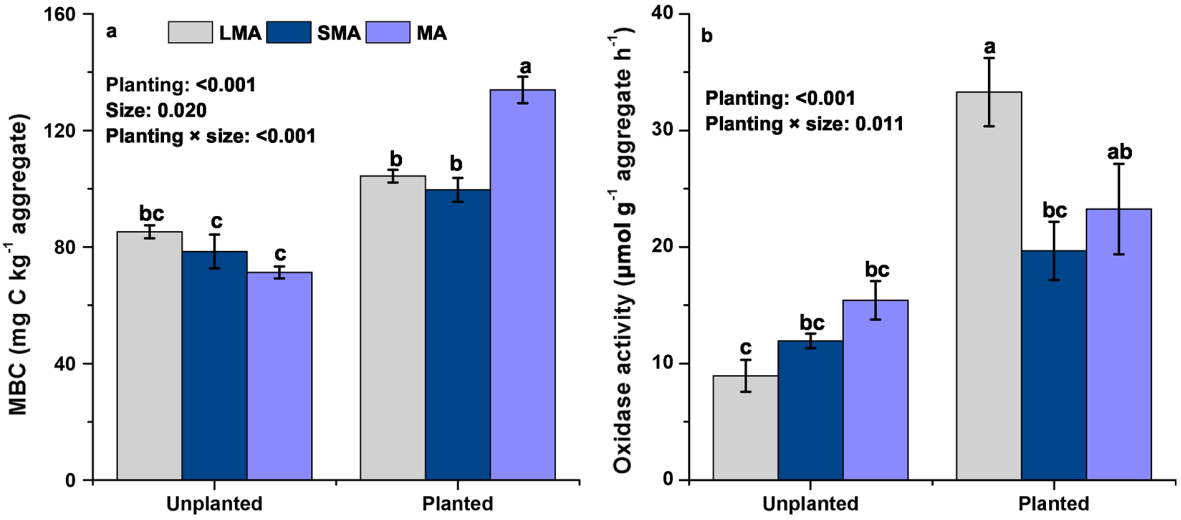

Fig. 3. Soil microbial biomass C (MBC, a) and oxidase (PO + PER) activity (b) in the three aggregate treatments with or without planting at the end of the experiment. Two-way ANOVA *P*-values are shown when significant ($P < 0.05$), and planting and size represent the effect of planting and aggregate size, respectively. Different lowercase letters indicate significant differences across all aggregates ($P < 0.05$). Error bars indicate standard errors of the mean, $n = 4$ for each treatment. For the abbreviations of soil aggregates, please see Table 1.

SOC (Jastrow et al. 2007). Supporting our first hypothesis, the lower RPE in the SMA treatment than in the other treatments for the first time provides empirical evidence that RPEs vary among aggregate size classes. While in a recent study the priming effects in aggregate size classes were explored by adding glucose (Tian et al. 2015), to our knowledge, our study is the first investigation on the effect of living roots.

Effects of plant-induced changes in net N immobilization and microbial activities on RPE

In contrast to several previous studies (Dijkstra et al. 2006, Zhu and Cheng 2012, Shahzad et al. 2015, Yin et al. 2018), we did not find any positive relationship between the plant biomass and root-derived CO_2 and RPE. In line with previous studies (Donald et al. 1987, Alexander and Miller 1991), the aggregate size class treatments altered plant growth. Plant biomass was highest in the SMA treatment (Table 2), and we therefore expected the highest rhizodeposition and RPE in this treatment. However, we actually observed the opposite result (Fig. 1b). This result suggests that the difference in RPEs among different aggregates could not be simply explained by the altered plant growth.

Supporting our second hypothesis, the positive relationship between the RPE and plant-induced changes in net N mineralization (Fig. 5a) suggests that an increase in microbial net N immobilization could decrease the positive RPE. Similar results were also found by Yin et al. (2018) and Lu et al. (2018). Lu et al. (2018) proposed a hypothesis that when soil is dominated by N immobilization, the RPE could decrease with increasing rhizodeposition. The highest plant-induced changes in net N immobilization and plant biomass, and the lowest RPE observed in the SMA treatment (Table 2, Figs. 1b, 2d) confirmed this hypothesis.

By providing labile C to rhizosphere microbes, it has been suggested that plants can accelerate microbial decomposition of N-enriched SOM (particularly of mineral associated organic matter) and convert the unavailable organic N into available inorganic N forms to plants (i.e., priming on gross N mineralization; Cheng et al. 2014, Jilling et al. 2018). Several studies have found a positive relationship between the primed gross N mineralization and RPE (Dijkstra et al. 2009, Bengtson et al. 2012, Zhu et al. 2014, Yin et al. 2018). However, an increased primed gross N mineralization does not always lead to positive

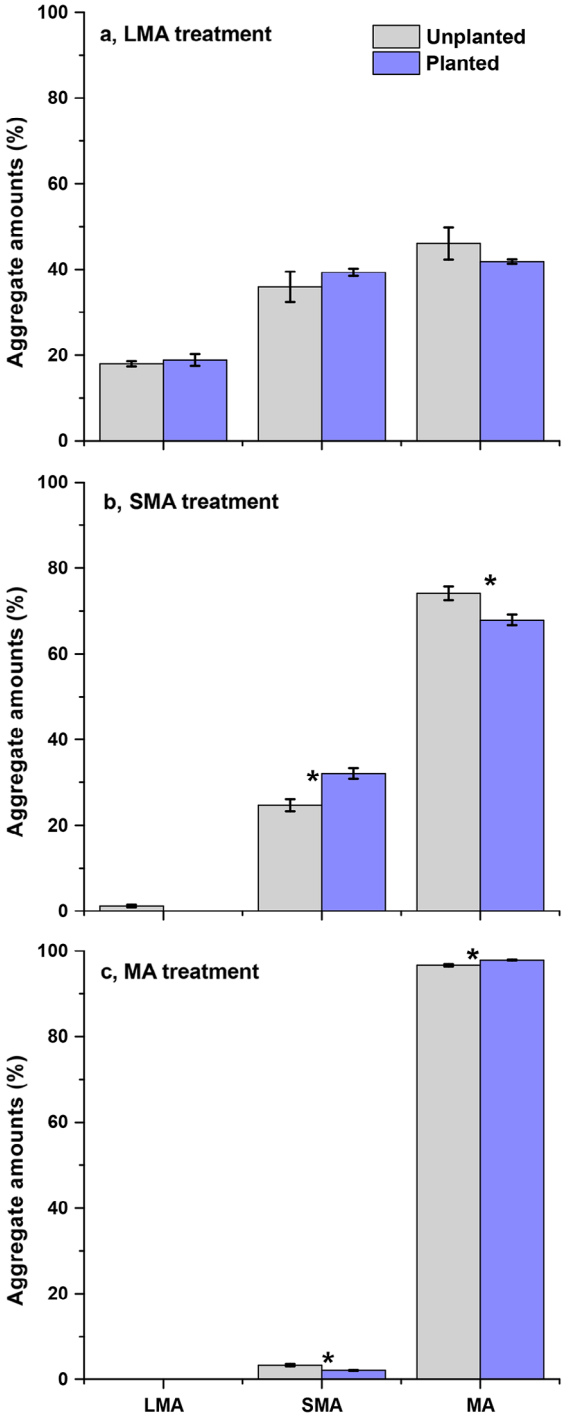

Fig. 4. Aggregate size redistribution (%) in each aggregate treatment. Error bars indicate standard errors of the mean, n = 4 for each treatment. For the abbreviations of soil aggregates, please see Table 1.

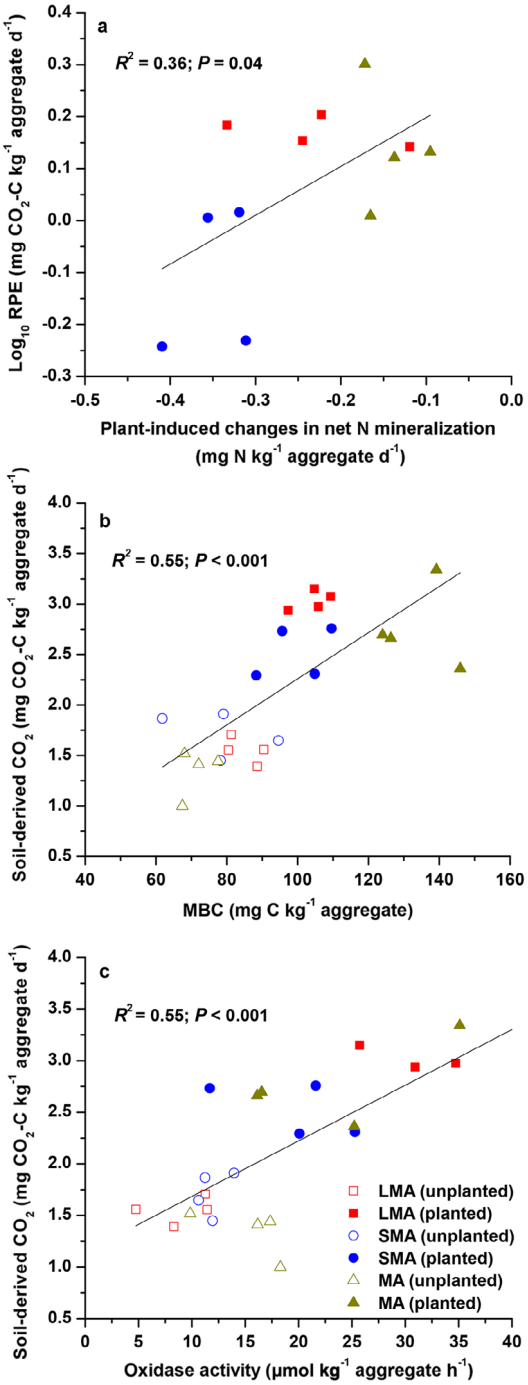

Fig. 5. Relationships between excess net N mineralization and RPE (log_{10} transformed, a), soil-derived CO_2 and MBC (b), and oxidase (PO + PER) activity (c). For the abbreviations of soil aggregates, please see Table 1. Data for (a), (b), and (c) include the unplanted controls (open symbols) and planted treatments (filled symbols), respectively (n = 4 for each treatment).

plant-induced changes in net N mineralization, since microbes have a higher efficiency in competing for N than plants, which can result in net N immobilization (Cheng 2009, Dijkstra et al. 2009, Yin et al. 2018). In our current study, the enhanced net N immobilization in all planted treatments indicates that the potential increased available N is more assimilated by microbes rather than taken up by plants (Fig. 2c). Therefore, in the SMA treatment, plants experienced a relatively higher N limitation, which may have to increase belowground C investment (Lu et al. 2018), that is, increases in root biomass. However, the RPE, plant-induced changes in net N mineralization, and rhizodeposition showed discordant changes in all aggregate treatments (e.g., the MA and LMA treatments, Table 2, Figs. 1b, 2d), suggesting that other factors like microbial activities may have regulated the variation in RPEs.

As expected, the microbial biomass and oxidase activity in all aggregate treatments were increased by planting (Fig. 3) and these increases positively influenced the RPEs (Fig. 5b, c), supporting our second hypothesis. The positive relationships have also been found by Lu et al. (2019) and can be explained by the microbial activation hypothesis: root-released labile C providing a readily C source for microbial growth, which then can accelerate SOM decomposition through the co-metabolism (Cheng and Kuzyakov 2005).

Noticeably, our results suggest that the difference in RPEs among different aggregates could partly be attributed to the various increases in MBC and oxidase activity (Fig. 3a, b). The largest increase in MBC induced by plants was found in the LMA treatment, while the largest oxidase activity was observed in the MA treatment (Fig. 3a, b). Rhizodeposition can be rapidly adsorbed to the surface of microaggregates due to their larger specific surface area (Totsche et al. 2018), which not only can directly relieve microbial C limitation and activate microbes in microaggregates, but also can liberate mineral-protected C and N through organic acids (e.g., oxalic acid) breaking the mineral–organic compounds (Keiluweit et al. 2015, Jilling et al. 2018). These processes may substantially enhance SOC decomposition through microbial activation (Cheng and Kuzyakov 2005). However, the highest increase in oxidase activity, accompanied by smaller increases in MBC in the LMA treatment, suggests that microbial assimilated rhizodeposits were used to synthesize oxidase to depolymerize recalcitrant SOM rather than to increase biomass, which can also lead to the relatively higher RPE (Zhu et al. 2014, Yin et al. 2018). Possibly, because of the relative lower MBC and oxidase activity, the RPE was lower in the SMA treatment (Figs. 1b, 3).

Effects of aggregate dynamics on the RPEs

Planting caused various impacts on aggregate dynamics differing in size classes (Fig. 4). As the

	Plant-induced changes in				RPE
	Net N mineralization	MBC	Oxidase activity	Aggregate destruction	
LMA	⊖	-	⊕	-	⊕
SMA	⊖	⊕	-	⊖	⊕
MA	⊖	⊕	-	⊕	⊕

Fig. 6. Plant-induced changes in soil variables (net N mineralization, MBC, oxidase activity, and aggregate destruction) and the RPE in different aggregate size classes. The signals (+ and −) in the circles indicate significant positive and negative planting effects, respectively. The size of the circles reflects the relative magnitude of the plant-induced changes.

effect of living roots on aggregate dynamics is mixed with formation, stabilization, and destruction (Six et al. 2004, Morris et al. 2019), our results suggests that the final impact of living roots on aggregate dynamics depends on aggregate size class, which differs in stability, porosity, and density (Materechera et al. 1994, De Gryze et al. 2005). The reduced destruction of SMA in the SMA treatment by planting (Fig. 4b) indicates that the formation and stabilization by root entanglement and rhizodeposition overcome the destruction by root penetration and dry–wet cycles. However, aggregates in the MA treatment changed little, while living roots only slightly reduced the formation of SMA (Fig. 4c). We speculate that the low SOC content in this treatment (Table 1) may have led to this lack of change, since organic matter is the main skeleton for microaggregates to build macroaggregates (Tisdall and Oades 1982, Blanco-Canqui and Lal 2004).

In the presence of living roots, the effect of aggregate dynamics on SOC decomposition lacks empirical evidence and only one hypothesis has been proposed, that is, the aggregate destruction hypothesis (Kuzyakov 2002, Cheng and Kuzyakov 2005). The aggregate destruction hypothesis suggests that an increase in aggregate destruction induced by living roots would enhance the RPE because of the release of microbial inaccessible aggregate-protected C. In the current study, the reduced destruction, the lower increase in microbial activities, and the lower RPE in the SMA treatment (Figs. 2b and 4b) than in the other treatments indirectly supported this hypothesis (Figs. 1b and 2). Furthermore, in the MA treatment, although we were unable to identify whether living roots break the microaggregates into even smaller aggregates (i.e., silt and clay fraction), the reduced formation of SMA by planting relative to the unplanted control in this treatment (Fig. 5c) suggests that planting destroyed some newly formed SMA, which indirectly supports the aggregate destruction hypothesis.

Although we have separately discussed the effect of plant-induced changes in net N mobilization, microbial activities, and aggregate dynamics on RPE, we could not directly distinguish the relative importance of these alterations in this study (Fig. 6). In reality, these plant-induced changes may operate individually or in combination, and there are most likely internal linkages among these changes (Cheng and Kuzyakov 2005, Lu et al. 2019). However, combined with findings of previous studies (Yin et al. 2018, Lu et al. 2019), our results suggest that enhanced microbial activity may account for variation in the RPE more than changes in net N mobilization or aggregate dynamics, because both changes in soil N mineralization and aggregate dynamics would ultimately work by microbial activities (Cheng et al. 2014).

Conclusion

Overall, by planting *Agropyron cristatum* in soil aggregates of different size classes, our results showed for the first time that positive RPEs caused by living roots varied with aggregate size classes. The lower RPE in the SMA treatment than in other treatments could be a result of the higher plant-induced net N immobilization, the lower increase in microbial activity, and the reduced aggregate destruction (Fig. 6). Given the complex impacts of living roots, we suggest that future studies should pay more attention to RPEs caused by living roots rather than simple exogenous C input. However, we only investigated the RPE by one species in isolated aggregates with different size classes. Under field conditions where all aggregates coexist and interplay, the role of aggregates on the RPE needs more specific research under different ecosystems. Our findings (Fig. 6) also imply the importance of plant–soil structure feedback in regulating soil C and N cycling which has often been ignored using a homogeneous soil.

Acknowledgments

We thank Jiayu Lu and Bo Fan for CO_2 trapping and destructive sampling. This work was supported by the National Key Research and Development Program (2015CB150802) and the National Natural Science Foundation of China (41601225 and 31500510).

Literature Cited

Alexander, K., and M. Miller. 1991. The effect of soil aggregate size on early growth and shoot-root ratio of maize (Zea mays L.). Plant and Soil 138:189–194.

Bengtson, P., J. Barker, and S. J. Grayston. 2012. Evidence of a strong coupling between root exudation, C and N availability, and stimulated SOM decomposition caused by rhizosphere priming effects. Ecology and Evolution 2:1843–1852.

Blanco-Canqui, H., and R. Lal. 2004. Mechanisms of Carbon Sequestration in Soil Aggregates. Plant Sciences 23:481–504.

Bond-Lamberty, B., and A. Thomson. 2010. Temperature-associated increases in the global soil respiration record. Nature 464:579–582.

Cheng, W. 2009. Rhizosphere priming effect: its functional relationships with microbial turnover, evapotranspiration, and C-N budgets. Soil Biology and Biochemistry 41:1795–1801.

Cheng, W., D. W. Johnson, and S. Fu. 2003. Rhizosphere effects on decomposition: controls of plant species, phenology, and fertilization. Soil Science Society of America Journal 67:1418–1427.

Cheng, W., and Y. Kuzyakov. 2005. Root effects on soil organic matter decomposition. Pages 119–143 *in* R. W. Zobel, and S. F. Wright, editors. Roots and soil management: interactions between roots and the soil, Agronomy Monograph no. 48. American Society of Agronomy, Crop Science Society of America, Soil Science Society of America, Madison, Wisconsin, USA.

Cheng, W., W. J. Parton, M. A. Gonzalez-Meler, R. Phillips, S. Asao, G. G. McNickle, E. Brzostek, and J. D. Jastrow. 2014. Synthesis and modeling perspectives of rhizosphere priming. New Phytologist 201:31–44.

De Gryze, S., J. Six, C. Brits, and R. Merckx. 2005. A quantification of short-term macroaggregate dynamics: influences of wheat residue input and texture. Soil Biology and Biochemistry 37:55–66.

Dijkstra, F. A., N. E. Bader, D. W. Johnson, and W. Cheng. 2009. Does accelerated soil organic matter decomposition in the presence of plants increase plant N availability? Soil Biology and Biochemistry 41:1080–1087.

Dijkstra, F. A., and W. Cheng. 2007. Moisture modulates rhizosphere effects on C decomposition in two different soil types. Soil Biology and Biochemistry 39:2264–2274.

Dijkstra, F., W. Cheng, and D. Johnson. 2006. Plant biomass influences rhizosphere priming effects on soil organic matter decomposition in two differently managed soils. Soil Biology and Biochemistry 38:2519–2526.

Donald, R., B. Kay, and M. Miller. 1987. The effect of soil aggregate size on early shoot and root growth of maize (Zea mays L.). Plant and Soil 103:251–259.

Dorodnikov, M., E. Blagodatskaya, S. Blagodatsky, S. Marhan, A. Fangmeier, and Y. Kuzyakov. 2009. Stimulation of microbial extracellular enzyme activities by elevated CO_2 depends on soil aggregate size. Global Change Biology 15:1603–1614.

Elliott, E. T. 1986. Aggregate structure and carbon, nitrogen, and phosphorus in native and cultivated Soils. Soil Science Society of America Journal 50:627–633.

Finzi, A. C., R. Z. Abramoff, K. S. Spiller, E. R. Brzostek, B. A. Darby, M. A. Kramer, and R. P. Phillips. 2015. Rhizosphere processes are quantitatively important components of terrestrial carbon and nutrient cycles. Global Change Biology 21:2082–2094.

Gupta, V. V., and J. J. Germida. 2015. Soil aggregation: influence on microbial biomass and implications for biological processes. Soil Biology and Biochemistry 80:A3–A9.

Huo, C., Y. Luo, and W. Cheng. 2017. Rhizosphere priming effect: a meta-analysis. Soil Biology and Biochemistry 111:78–84.

Jastrow, J. D., J. E. Amonette, and V. L. Bailey. 2007. Mechanisms controlling soil carbon turnover and their potential application for enhancing carbon sequestration. Climatic Change 80:5–23.

Jilling, A., M. Keiluweit, A. R. Contosta, S. Frey, J. Schimel, J. Schnecker, R. G. Smith, L. Tiemann, and A. S. Grandy. 2018. Minerals in the rhizosphere: overlooked mediators of soil nitrogen availability to plants and microbes. Biogeochemistry 139:103–122.

Keiluweit, M., J. J. Bougoure, P. S. Nico, J. Pett-Ridge, P. K. Weber, and M. Kleber. 2015. Mineral protection of soil carbon counteracted by root exudates. Nature Climate Change 5:588–595.

Keith, A., B. Singh, and F. A. Dijkstra. 2015. Biochar reduces the rhizosphere priming effect on soil organic carbon. Soil Biology and Biochemistry 88:372–379.

Kumar, A., M. Dorodnikov, T. Splettstößer, Y. Kuzyakov, and J. Pausch. 2017. Effects of maize roots on aggregate stability and enzyme activities in soil. Geoderma 306:50–57.

Kuzyakov, Y. 2002. Review: factors affecting rhizosphere priming effects. Journal of Plant Nutrition and Soil Science 165:382–396.

Lehmann, J., and M. Kleber. 2015. The contentious nature of soil organic matter. Nature 528:60–68.

Lu, J., F. A. Dijkstra, P. Wang, and W. Cheng. 2018. Rhizosphere priming of grassland species under different water and nitrogen conditions: a mechanistic hypothesis of C-N interactions. Plant and Soil 429:303–319.

Lu, J., F. A. Dijkstra, P. Wang, and W. Cheng. 2019. Roots of non-woody perennials accelerated long-term soil organic matter decomposition through

biological and physical mechanisms. Soil Biology and Biochemistry 134:42–53.

Materechera, S. A., J. M. Kirby, A. M. Alston, and A. R. Dexter. 1994. Modification of soil aggregation by watering regime and roots growing through beds of large aggregates. Plant and Soil 160:57–66.

Morris, E. K., D. J. P. Morris, S. Vogt, S. C. Gleber, M. Bigalke, W. Wilcke, and M. C. Rillig. 2019. Visualizing the dynamics of soil aggregation as affected by arbuscular mycorrhizal fungi. ISME Journal 13:1639–1646.

Murphy, C. J., E. M. Baggs, N. Morley, D. P. Wall, and E. Paterson. 2017. Nitrogen availability alters rhizosphere processes mediating soil organic matter mineralisation. Plant and Soil 417:499–510.

Passioura, J. B. 1991. Soil structure and plant growth. Soil Research 29:712–728.

Rabot, E., M. Wiesmeier, S. Schlüter, and H. J. Vogel. 2018. Soil structure as an indicator of soil functions: a review. Geoderma 314:122–137.

Shahzad, T., C. Chenu, P. Genet, S. Barot, N. Perveen, C. Mougin, and S. Fontaine. 2015. Contribution of exudates, arbuscular mycorrhizal fungi and litter depositions to the rhizosphere priming effect induced by grassland species. Soil Biology and Biochemistry 80:146–155.

Six, J., H. Bossuyt, S. Degryze, and K. Denef. 2004. A history of research on the link between (micro)aggregates, soil biota, and soil organic matter dynamics. Soil and Tillage Research 79:7–31.

Tian, J., J. Pausch, G. Yu, E. Blagodatskaya, Y. Gao, and Y. Kuzyakov. 2015. Aggregate size and their disruption affect 14C-labeled glucose mineralization and priming effect. Applied Soil Ecology 90:1–10.

Tisdall, J. M., and J. M. Oades. 1982. Organic matter and water-stable aggregates in soil. Journal of Soil Science 33:141–163.

Totsche, K. U., et al. 2018. Microaggregates in soils. Journal of Plant Nutrition and Soil Science 181:104–136.

Vance, E., P. Brookes, and D. Jenkinson. 1987. An extraction method for measuring soil microbial biomass C. Soil Biology and Biochemistry 19:703–707.

Wang, X., C. Tang, J. Severi, C. R. Butterly, and J. A. Baldock. 2016. Rhizosphere priming effect on soil organic carbon decomposition under plant species differing in soil acidification and root exudation. New Phytologist 211:864–873.

Yin, L., P. E. Corneo, A. Richter, P. Wang, W. Cheng, and F. A. Dijkstra. 2019. Variation in rhizosphere priming and microbial growth and carbon use efficiency caused by wheat genotypes and temperatures. Soil Biology and Biochemistry 134:54–61.

Yin, L., F. A. Dijkstra, P. Wang, B. Zhu, and W. Cheng. 2018. Rhizosphere priming effects on soil carbon and nitrogen dynamics among tree species with and without intraspecific competition. New Phytologist 218:1036–1048.

Zhu, B., and W. Cheng. 2012. Nodulated soybean enhances rhizosphere priming effects on soil organic matter decomposition more than non-nodulated soybean. Soil Biology and Biochemistry 51:56–65.

Zhu, B., and W. Cheng. 2013. Impacts of drying–wetting cycles on rhizosphere respiration and soil organic matter decomposition. Soil Biology and Biochemistry 63:89–96.

Zhu, B., J. L. M. Gutknecht, D. J. Herman, D. C. Keck, M. K. Firestone, and W. Cheng. 2014. Rhizosphere priming effects on soil carbon and nitrogen mineralization. Soil Biology and Biochemistry 76:183–192.